Removal of malachite green from aqueous solutions by electrocoagulation/peanut shell adsorption coupling in a batch system

Xiansheng Wang, Jiaheng Ni, Shuo Pang and Ying Li

ABSTRACT

A electrocoagulation (EC)/peanut shell (PS) adsorption coupling technique was studied for the removal of malachite green (MG) in our present work. The addition of an appropriate PS dosage (5 g/L) resulted in remarkable increase in the removal efficiency of MG at lower current density and shorter operating time compared with the conventional EC process. The effect of current density, pH of MG solution, dosage of PS and initial concentration of MG were also investigated. The maximum removal efficiency of MG was 98% under optimum conditions in 5 min. And it was 23% higher than that in EC process. Furthermore, the unit energy demand (UED) and the unit electrode material demand (UEMD) were calculated and discussed. The results demonstrated that the EC/PS adsorption coupling method achieved a reduction of 94% UED and UEMD compared with EC process.

Key words | adsorption, electrocoagulation, energy consumption, malachite green, peanut shell

Xiansheng Wang
Jiaheng Ni
Ying Li (corresponding author)
Key Laboratory of Groundwater Resources and Environment, Ministry of Education,
Jilin University,
Changchun 130026,
China
E-mail: *liying250403@jlu.edu.cn*

Shuo Pang
Changchun Inspection Center for Aquatic Products Safety and Quality,
Changchun 130026,
China

INTRODUCTION

Textile and tannery industries are some of the most contaminated in developed countries with 7×10^5 tons of dyestuffs produced annually (Asghar *et al.* 2015; Suárez-Escobar *et al.* 2015). Dyes are normally very large aromatic molecules consisting of many linked rings (Zodi *et al.* 2013). Dye molecules present a real threat to the environment and human health because of their structural stability and complexity (Njoku *et al.* 2014). The disposal of dye-containing water is currently a major problem from a global viewpoint (Ahmad *et al.* 2014). Various physical, physicochemical, and biological techniques were used to remove dyes from wastewater. Some of these processes include adsorption (Reddy *et al.* 2012; Dotto *et al.* 2015), coagulation–flocculation (Saitoh *et al.* 2014), filtration (Kajekar *et al.* 2015), electrocoagulation (EC) (Chafi *et al.* 2011), advanced oxidation (ozonation, Fenton's reagents, and UV radiation/hydrogen peroxide) (Bellebia *et al.* 2009), ion-exchange (Wu *et al.* 2008), biological treatment (Rodrigues *et al.* 2014) and air flotation (Liang *et al.* 2014).

The EC technique is considered to be a potentially effective method for wastewater treatment in past decades (Brillas & Martínez-Huitle 2015). EC is a process that involves creating flocs of metallic hydroxides within the effluent to be cleaned via electrodissolution of soluble anodes, usually aluminum or iron (Ricordel & Djelal 2014), and in a simultaneous reaction, hydroxyl ions and hydrogen gas are produced on the surface of the cathode, which leads to the production of various ferrous, ferric or Al (III) hydroxide, and polyhydroxy species, depending on the pH of the electrolyte (Kobya *et al.* 2011). The proposed mechanism for the generation of coagulation by using Al as an anode is presented below (de Carvalho *et al.* 2015a):

Mechanism 1:

$$\text{Anode: } Al_{(s)} \rightarrow Al^{3+}_{(aq)} + 3e^-$$
$$\text{In bulk: } Al^{3+}_{(aq)} + 3H_2O \rightarrow Al(OH)_3 + 3H^+_{(aq)}$$
$$\text{Cathode: } 3H^+_{(aq)} + 3e^- \rightarrow 3/2H_{2(g)}$$

Mechanism 2:

$$\text{Anode: } Al_{(s)} \rightarrow Al^{3+}_{(aq)} + 3e^-$$
$$\text{Cathode: } 3H_2O + 3e^- \rightarrow 3/2H_{2(g)} + 3OH^-_{(aq)}$$
$$\text{In bulk: } Al^{3+}_{(aq)} + 3OH^-_{(aq)} \rightarrow Al(OH)_3$$

The advantages of EC are a compact treatment facility, less sludge production, minimal requirement of chemicals and the possibility of complete automation (Hu *et al.* 2016). However, it is easy to form an impermeable oxide film on the cathode, which results in higher energy consumption and lower efficiency (Avsar *et al.* 2007; Secula *et al.* 2013). Hence, great efforts have been made to improve EC progress. Many studies showed that granular active carbon/EC coupling technique

doi: 10.2166/wst.2017.051

was more efficient and faster compared to conventional EC progress (Narayanan & Ganesan 2009; Secula *et al.* 2012a). As with active carbon, peanut shell (PS) is also a high surface area porous material with exceptional adsorptive properties. PS adsorption as an effective method to treat wastewater has been reported in various literature, such as removing methylene blue, brilliant cresyl blue, neutral red (Gong *et al.* 2005), heavy metals (Xu & Liu 2008; Witek-Krowiak *et al.* 2011) and organic compounds from aqueous solution. However, coupling the EC technique with PS adsorption was seldom reported before. PS is an effective and low-cost adsorbent and therefore ideal for application in developing countries.

In this work, we investigated the removal of malachite green (MG) from aqueous solution by EC/PS adsorption coupling method. PS was characterized by Fourier transform infrared spectroscopy (FTIR), scanning electron microscope (SEM) and pH_{pzc}. The effects of current density, dosage of PS, initial MG concentration and pH on the removal efficiency were discussed. The unit energy demand (UED) and the unit electrode material demand (UEMD) were also determined and discussed.

MATERIALS AND METHODS

Materials

Peanuts were purchased at a local market (Changchun, China) and were manually peeled immediately. PS was ground by a grinding mill and sieved to obtain a particle size range of 80 mesh. The powders were washed with distilled water for three times to remove the suspended solids and water-soluble materials. Then they were dried at 60 °C for 12 h. The dried PS were stored in plastic bottle for further use.

MG (C.I. No. 24000, $C_{23}H_{25}ClN_2$, MW = 364.91 g·mol^{-1}) was purchased from Shanghai Jinsui Bio-Technology Co., Ltd (Shanghai, China) (Figure 1).

The Na_2SO_4 was purchased from Xilong Chemical Co., Ltd (Shantou, China).

The H_2SO_4, HCl and NaOH were obtained from Beijing chemical works (Beijing, China).

EC/PS adsorption coupling experiments

The experiment was conducted in an EC cell of capacity 576 mL (12 cm × 4 cm × 12 cm) fabricated out of organic glass reactor. The bottom of the reactor was equipped with two perforated tubes to maintain uniform gas flow and stirring into the cell by using an aeration pump at 6 L·min^{-1}. Aluminum plate containing 99% aluminium was used as the anode and stainless steel

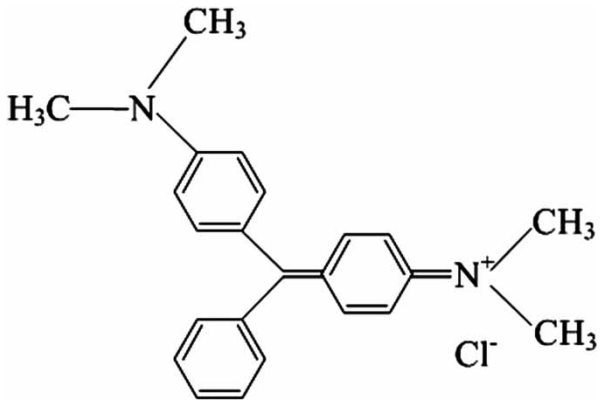

Figure 1 | The chemical structure of MG.

(SS-304) was used as the cathode. The effective electrode area was 20 cm^2. The anode and cathode were positioned vertically and parallel to each other with a gap. To adjust the conductivity, 1 g of Na_2SO_4 was dissolved in dye solutions (volume 1 L). Before each experiment, the electrodes were polished with fine-grained emery paper, washed with 1 N H_2SO_4 and then with distilled water. The experimental setup is shown in Figure 2.

For every experimental run, 400 mL of MG solution was placed into the reactor. The electrodes were connected to a digital DC power supply to obtain a constant current. The current density and electrode space were set to a desired value and then a certain quantity of PS was added to the solution. The pH was adjusted by adding 0.1 M HCl or 0.1 M NaOH and measured using a PHS-3E pH meter (Shanghai INESA and Scientific Instrument Co., Ltd, China). The experiments were performed at room temperature and the process was carried out for 1 h.

To assess the treatment process, a 2 mL water sample was drawn every 5 min during the experiment. The samples were filtrated by Whatman 0.45 μm filters, and then measured with a SDPTOP UV2600PC UV/VIS Spectrophotometer (Shanghai Sunny Hengping Scientific Instrument Co., Ltd, China) at a wavelength of 619 nm. The removal efficiency (Y (%)) of MG was calculated from:

$$Y = \frac{C_0 - C_t}{C_0} \times 100 \quad (1)$$

where C_0 is the concentration of MG before treated (g/L), and C_t is the concentration of MG after t min of treating (g/L).

Unit energy and electrode material consumption

Energy consumption is one of the vital parameters for the feasibility of the electrochemical process with a focus on EC, which deserves special attention from researchers in the area.

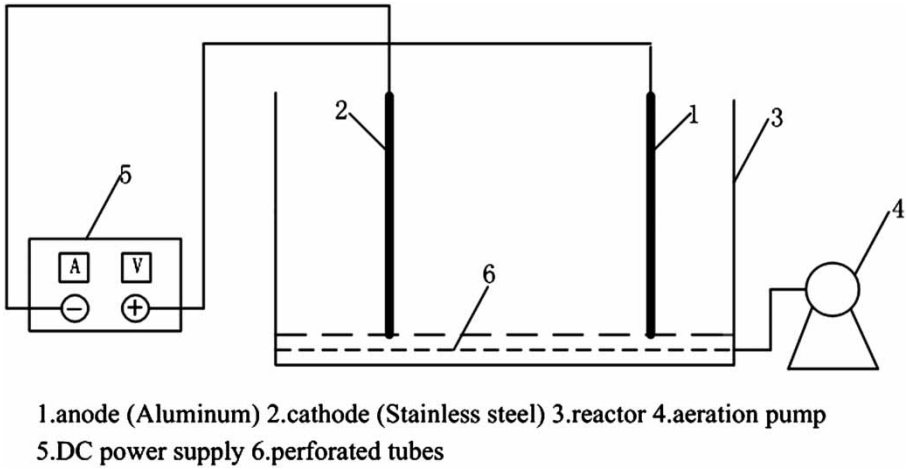

Figure 2 | Experimental set-up.

The experiments were carried out in a galvanostatic regime, and the cell voltage was varied during the traditional EC and EC/PS coupling process. Thus, the energy consumption related to the amount of removed dye, or UED (kWh/g) (Secula *et al.* 2012b), was calculated according to the following equation:

$$\mathrm{UED} = \frac{\mathrm{I}\cdot\int_0^t \mathrm{U}\cdot\mathrm{dt}}{\mathrm{V}\cdot\mathrm{C}_0\cdot\dfrac{\mathrm{Y_t}}{100}} \tag{2}$$

where U is the cell voltage, (V); I – current intensity, (A); t – time, (h); V – volume of MG solution, (L); Y_t – color removal efficiency at time t, (%).

The generation of the coagulant during the EC process leads to the consumption of the electrode material that can be estimated based on Faraday's law (Espinoza-Quiñones *et al.* 2009):

$$\mathrm{UEMD} = \frac{3600\cdot\mathrm{I}\cdot\mathrm{t}\cdot\mathrm{A}}{\mathrm{n}\cdot\mathrm{F}\cdot\mathrm{V}\cdot\mathrm{C}_0\cdot\dfrac{\mathrm{Y_t}}{100}} \tag{3}$$

where UEMD is the unit electrode material demand, (g/g); t – time, (h); n – number of electrons involved in the oxidation/reduction reaction; F – Faraday's constant, (C/mol); A – atomic mass of the electrode material, (g/mol).

Characterization methods

SEM measurements and energy dispersive X-ray (EDX) were performed by a field emission scanning electron microscope (Hitachi, S-4800) at an operating voltage of 3 kV and at an operating voltage of 20 kV, respectively. FTIR spectrums were obtained from a FT-IR spectrophotometer (Nicolet NEXUS470, Nicolet Co., Ltd, USA) with KBr disks. The point of zero charge (pHpzc) of PS was determined by batch equilibration method in which nine different solutions were prepared having pH values ranging from 2 to 10. At first, 20 cm^3 of distilled water was kept in several beakers and their pH values were adjusted by adding varying amounts of 0.1 mol/L of NaOH or HNO_3 solution. Then a portion of PS sample (50 mg) was added into beakers and kept for equilibration at room temperature. After 24 h, the final pH was measured and plotted as a function of initial pH values. The final pH value in the curve where a common plateau is obtained is the pH_{pzc} of the PS (Reddy *et al.* 2016).

RESULT AND DISCUSSION

Characterization of PS

SEM analysis

Figure 3 shows the SEM images of PS before and after MG adsorption. Figure 3(a) and 3(b) show PS surface before adsorption, it can be seen that PS presented an irregular, rough and porous surface which was good for adsorption. And it is clearly shown that MG had been adsorbed on the surface of PS after adsorption in Figure 3(c) and 3(d).

FTIR analysis

In order to examine the functional groups existing in PS, FTIR analysis was carried out. The FTIR spectrums of PS before

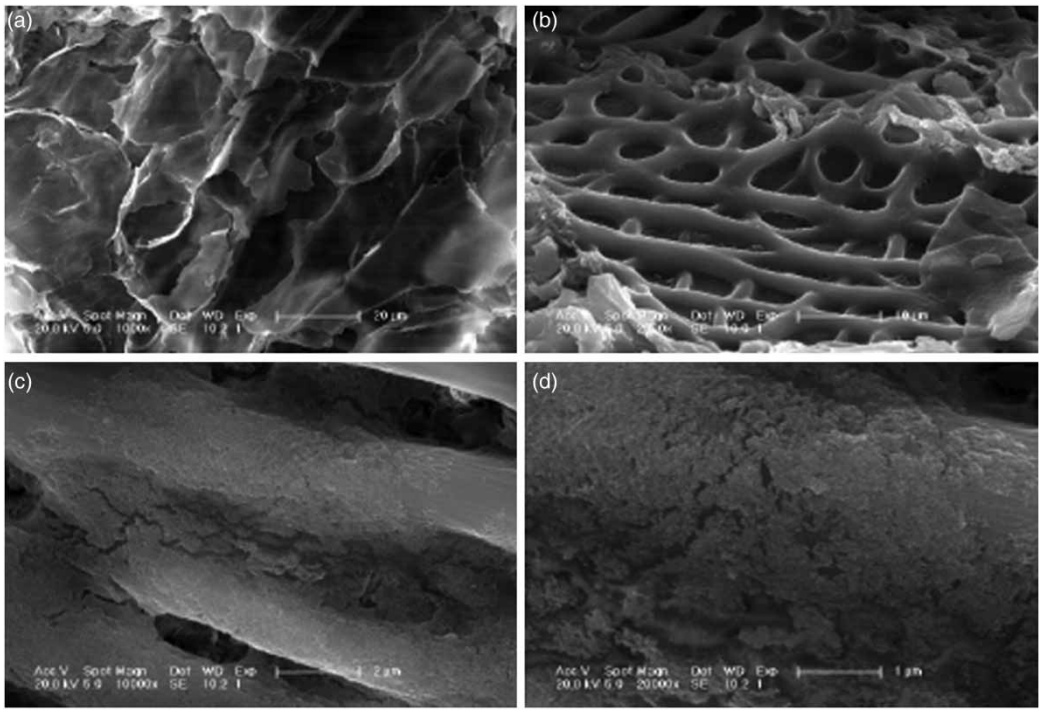

Figure 3 | The SEM images of PS before (a and b) and after (c and d) adsorption.

and after adsorption and MG are shown in Figure 4. For PS, the major intense bands were at 3,426 cm^{-1} (–OH stretching); 2,925 cm^{-1} (assigned to C–H stretching vibration); 1,630 cm^{-1} (carbonyl–C = O stretching vibration), attributed to carbonyl compounds, such as ketones, aldehydes alkenes, esters and C = C of aromatic groups; 1,260 cm^{-1}, possibly due to C–O, C–H or C–C stretching vibrations; 1,050 cm^{-1}, due to the C–O group in carboxylic and alcoholic groups.

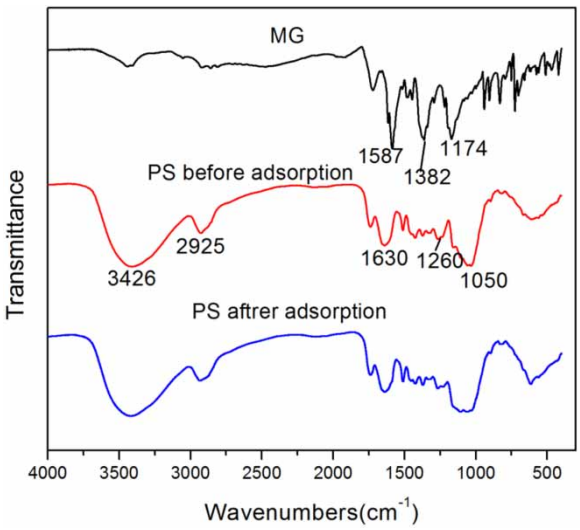

Figure 4 | FTIR spectra of MG, PS before and after adsorption.

Some of the above mentioned functional groups are typical of lignin, which is present in different agricultural wastes like PS (Georgin *et al.* 2016). For MG, the three characteristic absorption peaks at 1,587 cm^{-1}, 1,382 cm^{-1} and 1,174 cm^{-1} are C = C olefin structure stretching vibration, –C–N coterminous with the benzene ring structure stretching vibration and stretching vibration absorption of aromatic ring skeleton, respectively (GAO *et al.* 2011). Compared with the spectra for PS before adsorption, the peaks at 1,260 cm^{-1} and 1,050 cm^{-1} in the spectra for PS after adsorption disappeared, it indicated that the functional groups probably involved on the surface of the PS in adsorption process. In spite of this, a new peak was detected at 1,174 cm^{-1}, which was assigned to the C = C olefin structure stretching vibration in MG, indicating the adsorption of MG on the surface of PS.

pH_{pzc} of PS

pHpzc is the pH at which the surface exhibits net zero charge. The result is shown in Figure 5. It indicated that the pH_{pzc} is approximately 5.8, thus, adsorption of anionic dyes will be favored at $pH<pH_{pc}$ and at $pH>pH_{pzc}$ will favor the adsorption of cationic dyes. MG belongs to cationic dyes, so PS had a good adsorption capacity for MG in aqueous solution which has a pH > 5.8.

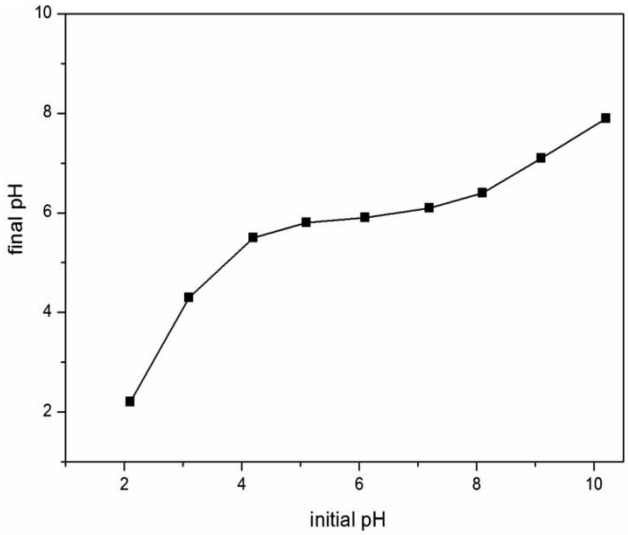

Figure 5 | pH_{PZC} of PS.

Effect of current density

The current density is determined by dividing each current by the corresponding electrode area. The effect of current density was studied at 1, 2, 3, 5 mA/cm^2. Figure 6 shows the removal efficiency studied in the two processes. The current density strongly determines the formation rate of flocculant (Chou 2010). In Figure 6(a), as the current density increased, the removal efficiency of MG also increased in traditional EC process. At high current density, the anodic dissolution of Al increased, which leads to an increase in the amount of metal hydroxides and resulted in an improvement of removal efficiency. Compared with the traditional EC process, adding PS could enhance the removal efficiency of MG signally in the same current density. Even at low current density value, the EC/PS coupling technique could achieve a fairly high removal efficiency in short time. As shown in Figure 6(b), the removal efficiency was 98% in 5 min. The high removal efficiency can be attributed to the fact that the system suffered both reactions simultaneously, EC and also adsorption process (de Carvalho *et al.* 2015b). Therefore, a current density of 2 mA/cm^2 was chosen as ideal during subsequent experiments.

Effect of PS dosage

The effect of PS dosage was studied with different PS concentrations ranging from 1 to 7 g/L. The other operational parameters were kept constant. The results are presented in Figure 7. It was observed that the removal efficiency of MG became significantly higher and the contact time for obtaining 98% removal efficiency decreases until 5 min with the increase in PS dosage from 0 to 5 g/L. The increasing PS dosage leads to more amounts of adsorbent and, thus, more surface area and active sorption sites, thereby leading to have more adsorbing capacity of MG (Ghaedi *et al.* 2014). This trend kept up to 5 g/L dosage, after that, the removal efficiency was almost stability until 7 g/L. So the optimum value of PS dosage was 5 g/L and was used for the rest of the study.

Effect of initial pH

To examine the effect of pH, the pH value of solution was adjusted to the range of 4–8 with other parameters

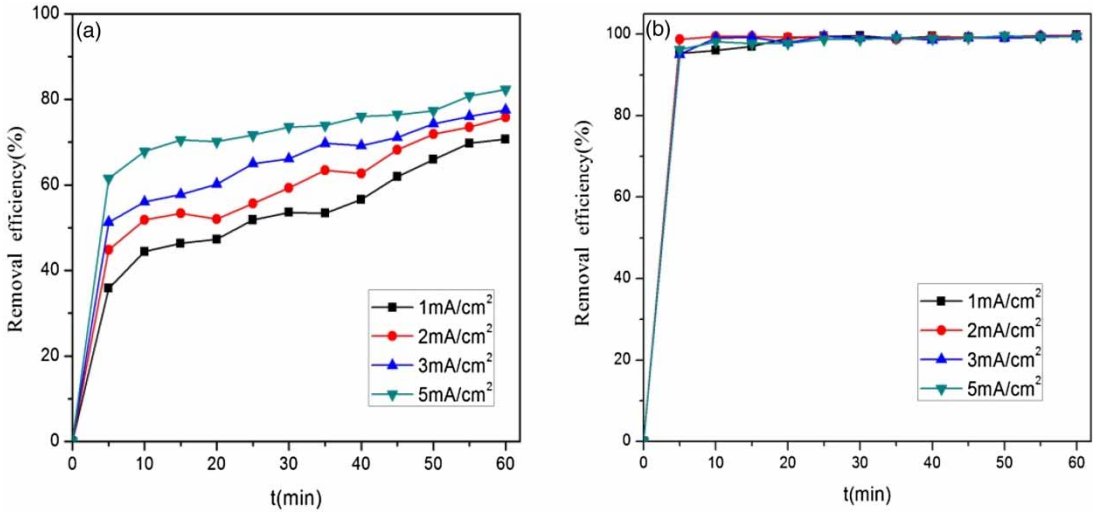

Figure 6 | Effect of current density without PS (a),with 5 g/L PS (b). $[MG]_0 = 50$ mg/L, $[Na_2SO_4] = 1$ g/L.

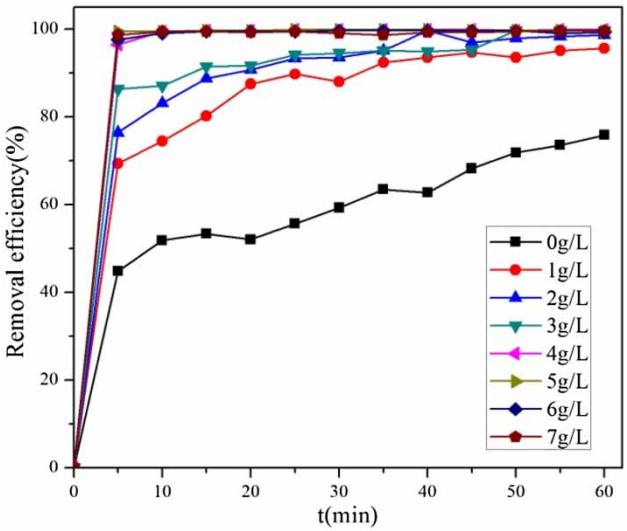

Figure 7 | Effect of PS dosage. $[MG]_0 = 50$ mg/L, $[Na_2SO_4] = 1$ g/L, CD = 2 mA/cm^2.

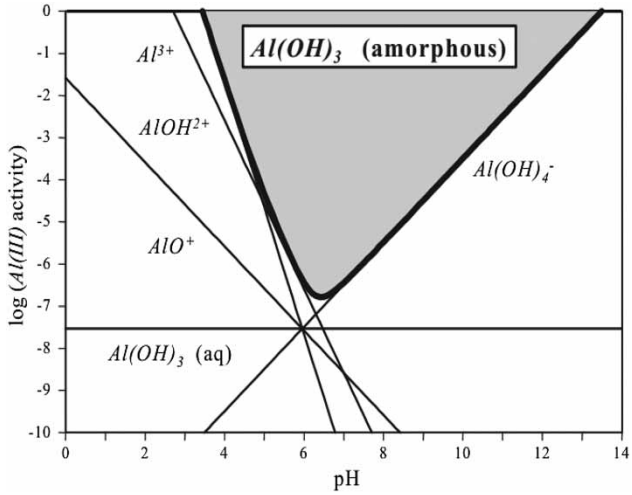

Figure 9 | Activity–pH diagram for Al(III) species in equilibrium with $Al(OH)_3$ (amorphous).

constant. The removal efficiency is shown in Figure 8. The result revealed that when pH of the MG solutions were higher than 6, the removal efficiency was much higher. pH of the solution could affect the surface charges of the PS, as well as the forms of metal hydroxides in aqueous solutions (Taşar *et al.* 2014). Figure 9 (Jiang *et al.* 2002) demonstrates different forms of $Al(OH)_3$ relative to the pH and concentration of Al^{3+} ions in the media. When pH of solution was too high or too low, $Al(OH)_3$ was in its charged form and soluble in water which could not be used for EC. When pH was neutral, $Al(OH)_3$ is stable and insoluble in the water and available for pollutant adsorption from water. On the other hand, combined with Figure 5, PS had a good adsorption capacity for MG in aqueous solution which has a pH > 5.8. According to the above analysis, we can conclude that the optimum pH for EC/PS adsorption coupling technique to removal MG is above 6. The pH of MG aqueous solution was at the range of 6.5–7, so other experiments were conducted without pH adjusting.

Effect of initial MG concentration

The initial concentration of MG on the coupling method removal efficiency was investigated, and the result is shown in Figure 10. We observed that an increase in dye

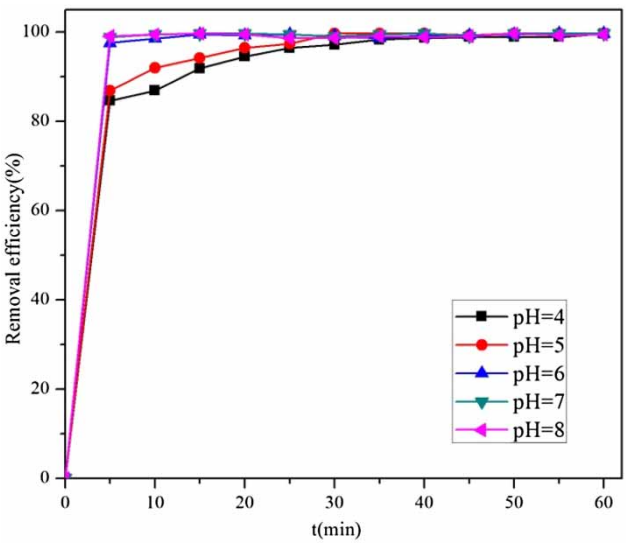

Figure 8 | Effect of pH. $[MG]_0 = 50$ mg/L, $[Na_2SO_4] = 1$ g/L, [PS] = 5 g/L, CD = 2 mA/cm^2.

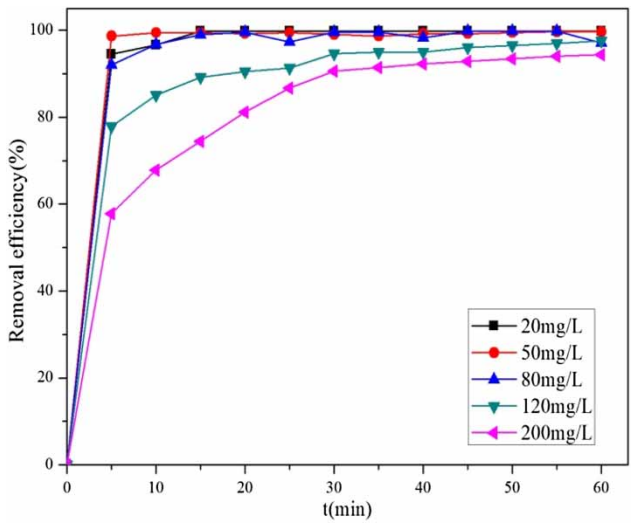

Figure 10 | Effect of initial MG concentration. $[Na_2SO_4] = 1$ g/L, [PS] = 5 g/L, CD = 2 mA/cm^2.

initial concentration caused a slightly reduction in removal efficiency. But the treatment time required to reach a removal of 94% of MG was 5, 5, 10, 30 and 60 min for concentrations of 20, 50, 80, 120 and 200 mg/L. According to Faraday's law, a constant amount of metal hydroxides is dissolved from the iron anode and passes to the solution for the same current density and operating time for all MG concentrations. Consequently, the same amount of metal hydroxides is produced in the aqueous solution. With increasing dye initial concentration while keeping the amount of PS constant and the amount of hydroxyl and metal ions produced on the electrodes at a constant current density, the adsorption capacity of the flocs and PS becomes insufficient and a reduction in the color removal conversion occurred at high MG concentrations (Parsa *et al.* 2011).

UED and UEMD analysis

UED was calculated from Equation (2). Figure 11(a) presents the UED values of different operation times in the EC process. The values were between 0.93 and 6.42 kWh/g and the removal efficiency was 75% in 60 min. While adding 5 g/L PS, the removal efficiency reached 98% in 5 min, and the UED was 0.34 kWh/g. Compared with the EC process, the removal efficiency improved 23% and UED reduced 94% using the coupling technique.

UEMD represents the consumption of electrode material in relation to the mass unity of removed dye as defined by Equation (3). Figure 11(b) shows the UMED of EC process. The values varied from 0.06 to 0.45 g/g in EC process while it was 0.02 g/g in EC/coupling technique. Same as UED, UMED reduced 94% in EC/PS adsorption coupling system compared with that in EC system.

Mechanism analysis

The removal efficiency of MG in 5 min in traditional EC process and EC/PS adsorption coupling process were 43% and 98%, respectively. The removal efficiency improved 51% due to the addition of PS. Removal of MG by PS adsorption was conducted to investigate the intensification mechanisms, and the result is shown in Figure 12. It can be seen that PS was a fast adsorbing material and the removal efficiency was 64% in 5 min. So the possible reason was that the EC method and the PS adsorption method worked together and promoted each other in the EC/PS adsorption coupling process.

CONCLUSION

From our present study, it was found that the removal of MG by the EC/PS adsorption coupling method is a feasible process. The addition of PS as adsorbent resulted in remarkable increase in the removal efficiency of MG at lower current density and operating time than the traditional EC process. The optimal conditions for the EC/PS coupling technique were as follows: current density was 2 mA/cm^2, dosage of PS was 5 g/L, initial MG concentration was 50 mg/L with an initial pH of solutions around neutral. Under optimal conditions, the optimal removal efficiency of MG was found to be 98% in 5 min, which was 23% higher than that in the EC process in 60 min. The energy

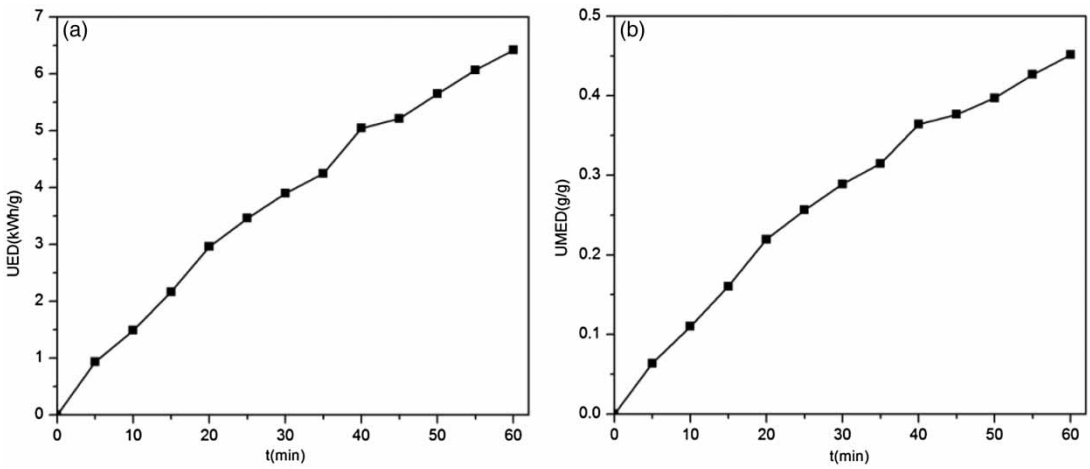

Figure 11 | UED (a) and UMED (b) in EC process.

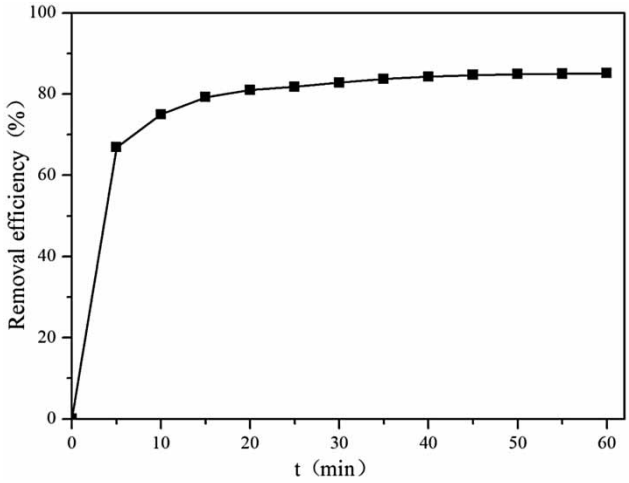

Figure 12 | Removal efficiency of MG by PS adsorption. $[MG]_0 = 50$ mg/L, $[Na_2SO_4] = 1$ g/L, $[PS] = 5$ g/L.

consumption and unit material energy consumption were 94% lower in the coupling process than that in the traditional EC process. Compared with similar state-of-the-art materials and method to treat MG, such as spent tea leaves activated carbon adsorption (Akar *et al.* 2013), almond shell adsorption (Ozdes *et al.* 2010) and poultry feather adsorption process (Beak *et al.* 2010), the EC/PS adsorption coupling method is the most efficient and cost-optimal method. Thus, we could conclude that the EC/PS adsorption coupling technique for MG removal is considerably cheaper, and is suitable for developed and developing countries.

ACKNOWLEDGEMENTS

This work was supported by the National Natural Science Foundation of China (No. 51308252), Jilin Province Science and Technology Development Plans (No. 20130101091JC) and the analysis and Changchun Technology Innovation Fund (No. 2009086).

REFERENCES

Ahmad, M. A., Puad, N. A. A. & Bello, O. S. 2014 Kinetic, equilibrium and thermodynamic studies of synthetic dye removal using pomegranate peel activated carbon prepared by microwave-induced KOH activation. *Water Resources and Industry* **6**, 18–35.

Akar, E., Altinişik, A. & Seki, Y. 2013 Using of activated carbon produced from spent tea leaves for the removal of malachite green from aqueous solution. *Ecological Engineering* **52**, 19–27.

Asghar, A., Raman, A. A. A. & Daud, W. M. A. W. 2015 Advanced oxidation processes for in-situ production of hydrogen peroxide/hydroxyl radical for textile wastewater treatment: a review. *Journal of Cleaner Production* **87**, 826–838.

Avsar, Y., Kurt, U. & Gonullu, T. 2007 Comparison of classical chemical and electrochemical processes for treating rose processing wastewater. *Journal of Hazardous Materials* **148** (1), 340–345.

Beak, M. H., Ljagbemi, C. O. & Kim, D. S. 2010 Treatment of malachite green-containing wastewater using poultry feathers as adsorbent. *Journal of Environment Science and Health Part A* **44** (5), 536–542.

Bellebia, S., Kacha, S., Bouberka, Z., Bouyakoub, A. & Derriche, Z. 2009 Color removal from acid and reactive dye solutions by electrocoagulation and electrocoagulation/adsorption processes. *Water Environment Research* **81** (4), 382–393.

Brillas, E. & Martínez-Huitle, C. A. 2015 Decontamination of wastewaters containing synthetic organic dyes by electrochemical methods. An updated review. *Applied Catalysis B: Environmental* **166**, 603–643.

Chafi, M., Gourich, B., Essadki, A., Vial, C. & Fabregat, A. 2011 Comparison of electrocoagulation using iron and aluminium electrodes with chemical coagulation for the removal of a highly soluble acid dye. *Desalination* **281**, 285–292.

Chou, W.-L. 2010 Removal and adsorption characteristics of polyvinyl alcohol from aqueous solutions using electrocoagulation. *Journal of Hazardous Materials* **177** (1), 842–850.

de Carvalho, H. P., Huang, J., Ni, J., Zhao, M., Yang, X. & Wang, X. 2015a Removal of Acid Black 1 and Basic Red 2 from aqueous solutions by electrocoagulation/*Moringa oleifera* seed adsorption coupling in a batch system. *Water Science and Technology* **72** (2), 203–213.

de Carvalho, H. P., Huang, J., Zhao, M., Liu, G., Dong, L. & Liu, X. 2015b Improvement of methylene blue removal by electrocoagulation/banana peel adsorption coupling in a batch system. *Alexandria Engineering Journal* **54** (3), 777–786.

Dotto, G., Santos, J., Rodrigues, I., Rosa, R., Pavan, F. & Lima, E. 2015 Adsorption of methylene blue by ultrasonic surface modified chitin. *Journal of Colloid and Interface Science* **446**, 133–140.

Espinoza-Quiñones, F. R., Fornari, M. M., Módenes, A. N., Palácio, S. M., da Silva, F. G., Szymanski, N., Kroumov, A. D. & Trigueros, D. E. 2009 Pollutant removal from tannery effluent by electrocoagulation. *Chemical Engineering Journal* **151** (1), 59–65.

Gao, R.-Q., Wang, Y.-Y., Zhang, R.-T., Wang, Y. & Quan, J.-J. 2011 Study on decolorization of fly ash-based porous ceramics for malachite green. *Bulletin of the Chinese Ceramic Society* **6**, 022.

Georgin, J., Dotto, G. L., Mazutti, M. A. & Foletto, E. L. 2016 Preparation of activated carbon from peanut shell by conventional pyrolysis and microwave irradiation-pyrolysis to remove organic dyes from aqueous solutions. *Journal of Environmental Chemical Engineering* **4** (1), 266–275.

Ghaedi, M., Ansari, A., Habibi, M. & Asghari, A. 2014 Removal of malachite green from aqueous solution by zinc oxide nanoparticle loaded on activated carbon: kinetics and isotherm study. *Journal of Industrial and Engineering Chemistry* **20** (1), 17–28.

Gong, R., Li, M., Yang, C., Sun, Y. & Chen, J. 2005 Removal of cationic dyes from aqueous solution by adsorption on peanut hull. *Journal of Hazardous Materials* **121** (1–3), 247–250.

Hu, C., Wang, S., Sun, J., Liu, H. & Qu, J. 2016 An effective method for improving electrocoagulation process: optimization of Al 13 polymer formation. *Colloids and Surfaces A: Physicochemical and Engineering Aspects* **489**, 234–240.

Jiang, J.-Q., Graham, N., André, C., Kelsall, G. H. & Brandon, N. 2002 Laboratory study of electro-coagulation–flotation for water treatment. *Water Research* **36** (16), 4064–4078.

Kajekar, A. J., Dodamani, B., Isloor, A. M., Karim, Z. A., Cheer, N. B., Ismail, A. & Shilton, S. J. 2015 Preparation and characterization of novel PSf/PVP/PANI-nanofiber nanocomposite hollow fiber ultrafiltration membranes and their possible applications for hazardous dye rejection. *Desalination* **365**, 117–125.

Kobya, M., Gebologlu, U., Ulu, F., Oncel, S. & Demirbas, E. 2011 Removal of arsenic from drinking water by the electrocoagulation using Fe and Al electrodes. *Electrochimica Acta* **56** (14), 5060–5070.

Liang, C.-Z., Sun, S.-P., Li, F.-Y., Ong, Y.-K. & Chung, T.-S. 2014 Treatment of highly concentrated wastewater containing multiple synthetic dyes by a combined process of coagulation/ flocculation and nanofiltration. *Journal of Membrane Science* **469**, 306–315.

Narayanan, N. V. & Ganesan, M. 2009 Use of adsorption using granular activated carbon (GAC) for the enhancement of removal of chromium from synthetic wastewater by electrocoagulation. *Journal of Hazardous Materials* **161** (1), 575–580.

Njoku, V., Foo, K., Asif, M. & Hameed, B. 2014 Preparation of activated carbons from rambutan (*Nephelium lappaceum*) peel by microwave-induced KOH activation for acid yellow 17 dye adsorption. *Chemical Engineering Journal* **250**, 198–204.

Ozdes, D., Gundogdu, A., Duran, C. & Senturk, H. B. 2010 Evaluation of adsorption characteristics of malachite green onto almond shell (*Prunus dulcis*). *Separation Science and Technology* **45** (14), 2076–2085.

Parsa, J. B., Vahidian, H. R., Soleymani, A. & Abbasi, M. 2011 Removal of acid brown 14 in aqueous media by electrocoagulation: optimization parameters and minimizing of energy consumption. *Desalination* **278** (1), 295–302.

Reddy, M. S., Sivaramakrishna, L. & Reddy, A. V. 2012 The use of an agricultural waste material, Jujuba seeds for the removal of anionic dye (Congo red) from aqueous medium. *Journal of Hazardous Materials* **203**, 118–127.

Reddy, P. M. K., Verma, P. & Subrahmanyam, C. 2016 Bio-waste derived adsorbent material for methylene blue adsorption. *Journal of the Taiwan Institute of Chemical Engineers* **58**, 500–508.

Ricordel, C. & Djelal, H. 2014 Treatment of landfill leachate with high proportion of refractory materials by electrocoagulation: system performances and sludge settling characteristics. *Journal of Environmental Chemical Engineering* **2** (3), 1551–1557.

Rodrigues, C. S., Madeira, L. M. & Boaventura, R. A. 2014 Synthetic textile dyeing wastewater treatment by integration of advanced oxidation and biological processes–performance analysis with costs reduction. *Journal of Environmental Chemical Engineering* **2** (2), 1027–1039.

Saitoh, T., Saitoh, M., Hattori, C. & Hiraide, M. 2014 Rapid removal of cationic dyes from water by coprecipitation with aluminum hydroxide and sodium dodecyl sulfate. *Journal of Environmental Chemical Engineering* **2** (1), 752–758.

Secula, M. S., Cagnon, B., de Oliveira, T. F., Chedeville, O. & Fauduet, H. 2012a Removal of acid dye from aqueous solutions by electrocoagulation/GAC adsorption coupling: kinetics and electrical operating costs. *Journal of the Taiwan Institute of Chemical Engineers* **43** (5), 767–775.

Secula, M. S., Cretescu, I. & Petrescu, S. 2012b Electrocoagulation treatment of sulfide wastewater in a batch reactor: effect of electrode material on electrical operating costs. *Environmental Engineering and Management Journal* **11** (8), 1485–1491.

Secula, M. S., Cretescu, I., Cagnon, B., Manea, L. R., Stan, C. S. & Breaban, I. G. 2013 Fractional factorial design study on the performance of GAC-enhanced electrocoagulation process involved in color removal from dye solutions. *Materials* **6** (7), 2723–2746.

Suárez-Escobar, A., Pataquiva-Mateus, A. & López-Vasquez, A. 2015 Electrocoagulation – photocatalytic process for the treatment of lithographic wastewater. Optimization using response surface methodology (RSM) and kinetic study. *Catalysis Today* **266**, 120–125.

Taşar, Ş., Kaya, F. & Özer, A. 2014 Biosorption of lead (II) ions from aqueous solution by peanut shells: equilibrium, thermodynamic and kinetic studies. *Journal of Environmental Chemical Engineering* **2** (2), 1018–1026.

Witek-Krowiak, A., Szafran, R. G. & Modelski, S. 2011 Biosorption of heavy metals from aqueous solutions onto peanut shell as a low-cost biosorbent. *Desalination* **265**, 126–134.

Wu, J.-S., Liu, C.-H., Chu, K. H. & Suen, S.-Y. 2008 Removal of cationic dye methyl violet 2B from water by cation exchange membranes. *Journal of Membrane Science* **309** (1), 239–245.

Xu, T. & Liu, X. 2008 Peanut shell activated carbon: characterization, surface modification and adsorption of Pb^{2+} from aqueous solution. *Chinese Journal of Chemical Engineering* **16** (3), 401–406.

Zodi, S., Merzouk, B., Potier, O., Lapicque, F. & Leclerc, J.-P. 2013 Direct red 81 dye removal by a continuous flow electrocoagulation/flotation reactor. *Separation and Purification Technology* **108**, 215–222.

First received 28 April 2016; accepted in revised form 16 January 2017. Available online 1 February 2017